JOURNAL OF CATALYSIS 132, 343–359 (1991)

Phase Cooperation between Tin and Antimony Oxides in Selective Oxidation of Isobutene to Methacrolein

II. Impregnated Catalysts

L. T. WENG, B. YASSE, J. LADRIÈRE,* P. RUIZ, AND B. DELMON[1]

*Unité de Catalyse et Chimie des Matériaux Divisés, and *Unité de Chimie Inorganique et Nucléaire, Université Catholique de Louvain, Place Croix du Sud 1, 1348 Louvain-la-Neuve, Belgium*

Received March 26, 1990; revised February 26, 1991

The selectivity and yields for methacrolein in the oxidation of isobutene over pure SnO_2 and Sb_2O_4 can be improved dramatically by impregnating the oxides with a small amount of the cation belonging to the other oxide (Sb for SnO_2 and Sn for Sb_2O_4). The fresh and used samples were characterized with XRD, BET, ^{119}Sn Mössbauer spectroscopy, SEM, analytical electron microscopy (AEM), XPS, and ESR. For Sb_2O_4 impregnated with Sn ions, no trace of surface contamination (monolayer or otherwise) or solid solution was detected. For SnO_2 impregnated with Sb ions, a small amount of Sb^{5+} ions dissolved into SnO_2 after impregnation, but these Sb^{5+} ions tend to migrate to the surface during catalytic reaction. For both systems, the impregnated ions tended to segregate, leading to the formation of a two-phase catalyst. A remote control mechanism can satisfactorily explain the results obtained. In comparison with the results obtained with SnO_2–Sb_2O_4 mechanical mixtures reported in Part I, the impregnated catalysts have good catalytic performances, account taken of the small amount of the minor component. The difference between the catalytic properties (methacrolein yield and selectivity) of impregnated catalysts and those of mechanical mixtures can be easily explained by considering the surface areas developed and the difference in the number and quality of the contacts between the SnO_2 and Sb_2O_4.

INTRODUCTION

In Part I (*1*), we presented results on the activity of catalysts prepared by mechanically mixing Sb_2O_4 powder with SnO_2 powder as well as results of the physico-chemical characterization of these catalysts. It was shown that SnO_2 and Sb_2O_4 worked synergistically in the selective oxidation of isobutene to methacrolein. It was essentially the selectivity to methacrolein formation that was dramatically improved. Extensive characterization gave no indication of new phase formation (or solid solution) or mutual contamination between two oxides. The SnO_2–Sb_2O_4 mixtures are constituted of two separate oxide phases and the observed synergy was explained by a remote control mechanism. According to this mechanism, molecular oxygen is adsorbed on the surface of Sb_2O_4 and becomes dissociated into oxygen species (spillover oxygen). This mobile species migrates onto the surface of SnO_2 where it creates new selective catalytic sites for selective oxidation and/or regenerates the sites that eventually become deactivated during the oxidation reaction.

However, it has been proposed in the literature that the formation of a new phase or extensive surface contamination of one oxide by an element belonging to the other might occur easily in some systems and explain synergy. The most illustrative example concerns V_2O_5–TiO_2 (*2–4*). Much attention has been paid to the thermodynamics and kinetics of this contamination (*5, 6*). In this case, TiO_2 is extensively covered by V_2O_5, and no remote control mechanism is necessary to explain the observed results. The

[1] To whom correspondence should be addressed.

0021-9517/91 $3.00

synergy may be essentially due to the formation of the special surface species.

The aim of this paper is to investigate further whether the same phenomenon, namely surface contamination of one oxide by the other, could take place in the SnO_2–Sb_2O_4 system. In addition, the literature mentions the existence of solid solutions of Sb^{5+} in SnO_2. Our attention was therefore also directed to the possible effect of the formation of this solid solution in our experiments.

It is not easy to detect contamination if the phenomenon only involves small amounts of the second element. However, there is a possibility of indirectly arriving at convincing arguments against contamination. If we suppose that some contamination is created artificially and that the contamination diminishes or disappears during catalytic work, such an observation would constitute proof that there is little or even no tendency to mutual contamination. This is the kind of experiment we carried out in the work reported here.

Thus, the objectives of this paper are to study artificially contaminated samples (Sb_2O_4 contaminated by Sn ions or SnO_2 contaminated by Sb ions) and to see whether this contamination is stable under the conditions of catalytic reaction. We used impregnation to create contamination. The quantity of the impregnated metallic ions was calculated so that it would be theoretically sufficient to form between $\frac{1}{4}$ and 2 monolayers of the impregnated oxide over the other (the "support") (*7, 8*). In order to maximize the possibility of establishing a contamination and to avoid the sintering of the deposited phase, the impregnated samples were not calcined prior to the catalytic test. The fresh and used samples were characterized using BET surface area measurements, XRD, electron microscopy (SEM and analytical electron microscopy (AEM)), ^{119}Sn Mössbauer spectroscopy, ESR, and XPS. XRD, ^{119}Sn Mössbauer spectroscopy, and ESR were used to detect the possible formation of a solid solution of Sb^{5+} dissolved in SnO_2. An ESR signal ($g = 1.8733$) can be used as an indication of the incorporation of Sb^{5+} into SnO_2 (*9*). By detecting and measuring possible shifts of the XRD peak positions, it is theoretically possible to see if the Sb ions are incorporated in substantial proportions into SnO_2. The direction of the shift (lower or higher angle) would point to the incorporation of Sb^{5+} ions or Sb^{3+} ions because the diameters of these ions are quite different ($R_{Sb^{5+}}$ = 0.62 Å, $R_{Sn^{4+}}$ = 0.71 Å, $R_{Sb^{3+}}$ = 0.76 Å) (*10*). The XPS technique, in association with AEM, was used to detect the possible formation of monolayers or fractions of monolayers, or other sorts of surface contamination.

EXPERIMENTAL

Catalyst Preparation

(*1*) *Pure Oxides*

Pure Sb_2O_4 (2 $m^2\ g^{-1}$) and SnO_2 (9.0 $m^2\ g^{-1}$) were prepared by the methods described previously (*1*).

(*2*) *Impregnated Catalysts*

(*a*) *Sb_2O_4 impregnated by Sn^{2+} (or Sn^{4+}).* The quantity of SnO_2 necessary to form a monolayer on the surface of Sb_2O_4 can be estimated on the basis of the BET surface area of Sb_2O_4 (2 $m^2\ g^{-1}$). We take as a basis the deposition of the (100) face (0.084 nm^2 as approximately calculated from the unit cell of SnO_2 (*11*)) of SnO_2 on the surface of Sb_2O_4. The amount contained in one monolayer corresponds to 1.2 wt% of SnO_2. The preparation procedures are given below.

A solution with the calculated concentration of Sn^{2+} (or Sn^{4+}) was prepared from $SnCl_2 \cdot 2H_2O$ (or $SnCl_4 \cdot 4H_2O$). Five grams of Sb_2O_4 was mixed with the required amount of Sn^{2+} (or Sn^{4+}) solution in a rotavapor, to which 250 ml of distilled water was added. The solution thus obtained was evaporated slowly at about 60°C under reduced pressure with continuous agitation. The powder obtained was then washed with a very dilute aqueous NH_3 solution in order to eliminate the Cl^- ions (complete elimination was checked with $AgNO_3$ solution) and

dried overnight at 110°C. The catalysts were used as such, without calcination.

Sb_2O_4 catalysts impregnated with quantities of Sn^{4+} necessary to form $\frac{1}{4}$, $\frac{1}{2}$, 1, and 2 monolayers of SnO_2 over Sb_2O_4 were prepared. They are designated as XSn^{4+}/Sb_2O_4, where X refers to the number of monolayers. The sample prepared with $SnCl_2$ is indicated by $1Sn^{2+}/Sb_2O_4$.

(*b*) *SnO_2 impregnated by Sb^{3+} and Sb^{5+}.* Similarly, the quantity necessary for forming a monolayer of Sb_2O_4 over SnO_2 can be estimated assuming the deposition of molecules having the arrangement of the (100) face and the surface area of SnO_2 (9.0 $m^2\ g^{-1}$). (The surface of the (100) face of a unit cell of Sb_2O_4 (*12*) was estimated to be 0.16 nm^2). This calculated amount represents 4 wt% of Sb_2O_4. It is known that Sb_2O_4 is composed of an equal number of Sb^{3+} and Sb^{5+}. This is why a mixture of Sb^{3+} and Sb^{5+} was used for impregnation in our case. The preparation procedure is given below.

A solution containing Sb^{3+} and Sb^{5+} (Sb^{3+}/Sb^{5+} = 1/1) was prepared from $SbCl_3$ (Aldrich, 99%) and $SbCl_5$ (Aldrich, 99.5%). $CHCl_3$ (Union Chimique Belge, p.a.) was used as the solvent in this case because SnO_2 is not soluble in that solvent. The SnO_2 powder was immersed in the necessary amount of this solution in a rotavapor, with the addition of 250 ml $CHCl_3$. Evaporation of the solvent was performed very slowly under reduced pressure. The powder so obtained was washed with NH_3 solution in order to eliminate Cl^- (complete elimination was checked with $AgNO_3$ solution) and finally dried at 110°C overnight. The catalysts were used as such, without calcination.

Samples of SnO_2 impregnated with quantities of Sb^{3+} and Sb^{5+} necessary to form $\frac{1}{4}$, $\frac{1}{2}$, 1, and 2 monolayers of Sb_2O_4 on SnO_2, were prepared. These catalysts are designated hereafter as XSb/SnO_2, where X refers to the theoretical number of monolayers.

Catalyst Characterization

XRD measurements were carried out in a Siemens D-500 diffractometer. BET surface areas were measured using a Setaram MTB 10-8 microbalance. For SEM and AEM we used a Jeol Temscan 100 CX electron microscope and a Kevex 5100 C energy dispersive spectrometer. ^{119}Sn Mössbauer spectroscopy measurements were performed in a spectrometer with a $Ca^{119}SnO_3$ source. ESR experiments were realized in a X-band Varian-12 spectrometer. XPS spectra were obtained in a Vacuum Generators ESCA-3 instrument. Detailed descriptions of these techniques and data acquisition parameters are given in Part I (*1*). We have also indicated in Part I the limits of detection that can be expected for these various methods.

In the XPS measurements, we used two methods to interpret our results. The first is the one used in Part I (*1*) based on results with an external SiO_2 standard. We calculated the apparent relative surface concentrations of C_{Sn}/C_{Si} and C_{Sb}/C_{Si}, using the sensitivity factors proposed by Wagner *et al.* (*13*). The "apparent relative surface concentration," C_{Sn}/C_{Si} or C_{Sb}/C_{Si}, represents with a good approximation the surface exposed by each oxide (SnO_2 or Sb_2O_4). The reason for using an external reference, SiO_2, has been given previously (*1*). From the apparent relative surface concentrations we calculated the surface composition index, namely the fraction of the surface occupied by deposited element: $r_{XPS\text{-}Sn}$ = Sn/(Sn + Sb) for Sn/Sb_2O_4 and $r_{XPS\text{-}Sb}$ = Sb/(Sn + Sb) for Sb/SnO_2.

In the other method, we compared the real XPS intensity ratio ($\mathbf{I}_m/\mathbf{I}_s$) with that calculated theoretically for monolayer formation ($\mathbf{I}_m^0/\mathbf{I}_s^0$). $\mathbf{I}_m^0/\mathbf{I}_s^0$ was calculated using the equation proposed by Kerkhof and Moulijn (*14*):

$$\frac{\mathbf{I}_m^0}{\mathbf{I}_s^0} = \frac{n_m}{n_s}\frac{D_m}{D_s}\frac{\sigma_m}{\sigma_s}\frac{1}{\rho_s S_s \lambda_s} \times \frac{(1 + \exp\{-2/\rho_s \lambda_m S_s\})}{(1 - \exp\{-2/\rho_s \lambda_m S_s\})}. \quad (1)$$

In this equation, n_m/n_s is the atomic ratio of the elements representative of the supported phase (e.g., m for Sb in the case of Sb/SnO_2) and the support (s = Sn for Sb/

SnO_2). D_m and D_s are the spectrometer detection efficiencies for the corresponding photoelectrons. In our instrument, D is inversely proportional to electron kinetic energy. The photoelectron cross section σ_m and σ_s were taken from Scofield (*15*)

$$\sigma_{Sb_{3d_{3/2}}} = 11.13, \quad \sigma_{Sn_{3d_{5/2}}} = 14.63.$$

Photoelectron escape depths, λ_m and λ_s, were estimated using the method given by Szajman *et al.* (*16*)

$$\lambda_{Sn_{3d_{5/2}}} = 1.18\,\text{nm}, \quad \lambda_{Sb_{3d_{3/2}}} = 1.22\,\text{nm}.$$

ρ_s is the density of the support ($\rho_{SnO_2} = 6.95$ g·cm^{-3}, $\rho_{Sb_2O_4} = 5.82$ g·cm^{-3}). S_s is the specific surface of the support.

In the case where the impregnated oxide is present as discrete particles (e.g., as cubic crystallites), the XPS intensity ratio $\mathbf{I}_m/\mathbf{I}_s$ may be expressed as the function of the particle size and the XPS intensity ratio for monolayer formation $\mathbf{I}_m^0/\mathbf{I}_s^0$:

$$\frac{\mathbf{I}_m}{\mathbf{I}_s} = \frac{\mathbf{I}_m^0}{\mathbf{I}_s^0}\,\frac{1 - \exp(-c/\lambda_m)}{c/\lambda_m}, \qquad (2)$$

where c is the average edge length of the cubic crystallites. Using Eq. (2), it is possible to estimate the particle size c.

For the Sb/SnO_2 samples after the catalytic reaction, one difficulty for physicochemical characterization was the deposition of coke, as previously observed (*1*). In order to eliminate the deposited coke, the used catalysts were calcined in air at 400°C for 20 h. For the samples Sn/Sb_2O_4, however, no apparent deposition of coke was observed after reaction but the XPS measurements showed a decrease of the Sn concentration. We calcined some fresh samples in order to see if the decrease of Sn concentration was due to thermal treatment.

Catalytic Activity Measurements

Isobutene selective oxidation was carried out in a continuous-flow fixed-bed reactor. The reactor and analytical systems have been described in detail in Part I. The reactor is a glass tube with an internal diameter of 8 mm. It was packed with catalyst (particle size: 500–800 μm) in the center and two packing beds composed of glass pills (1000 μm) at the top and bottom. The reaction conditions were the following: isobutene/O_2/N_2 (diluting gas) = 1/2/7; total pressure, 760 mm Hg; reaction temperatures, 380–420°C; the total feed (isobutene + O_2 + N_2), 30 ml/min; catalyst weight 800 or 400 mg (see Ref. (*1*)).

The choice of reaction conditions and the experimental procedures have been described in detail in (*1*).

TABLE 1

Surface Areas of Impregnated Catalysts ($m^2\ g^{-1}$)

Samples	Before reaction	After reaction	After reaction + reg.[a]
$1Sn^{2+}/Sb_2O_4$	2.2	3.5	
$1Sn^{4+}/Sb_2O_4$	1.9	2.6	
$1Sn^{4+}/Sb_2O_4$ (400°C 6h)	2.9		
$\frac{1}{4}Sb/SnO_2$	8.9	9.8	
$1Sb/SnO_2$	9.1	9.8	
$2Sb/SnO_2$	9.8	10.7	10.5

[a] Reg. refers to the calcination of the sample at 400°C for 20 h (the surface areas of the Sb_2O_4 and SnO_2 are, respectively, 2 and 9.0 $m^2\ g^{-1}$).

RESULTS

1. Characterization

1.1. Surface Area

The BET surface areas of the impregnated catalysts are reported in Table 1. For Sb_2O_4 impregnated with Sn^{2+} or Sn^{4+} ions and taking into account the precision of BET measurement, the surface area was not modified during impregnation. However, the surface area increased after catalytic reaction or thermal calcination at 400°C for 6 h.

For SnO_2 impregnated with Sb ions, the surface area did not change for $\frac{1}{4}Sb/SnO_2$ and $1Sb/SnO_2$ after impregnation, while that of $2Sb/SnO_2$ seemed to increase slightly (9.0 m^2/g for pure SnO_2 and 9.8 m^2/g for $2Sb/SnO_2$). Similar to Sn/Sb_2O_4, the surface area significantly increased after catalytic reac-

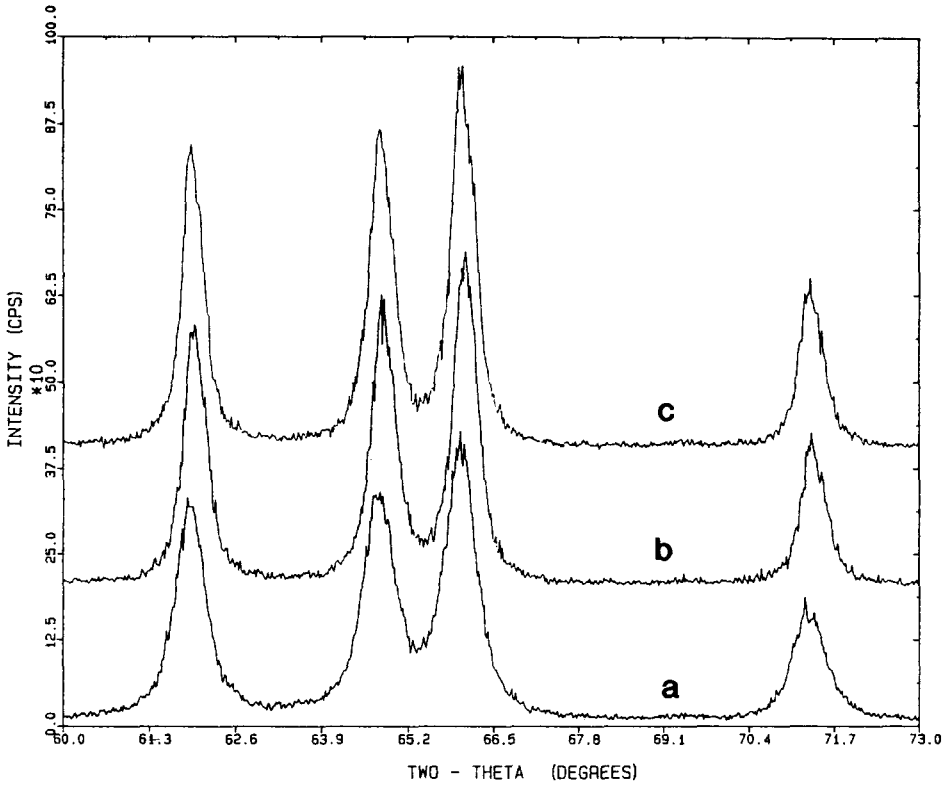

FIG. 1. X-ray diffraction spectra for $\frac{1}{2}Sb/SnO_2$, (a) SnO_2, (b) $\frac{1}{2}Sb/SnO_2$, and (c) $\frac{1}{2}Sb/SnO_2$ after reaction.

tion. However, when the sample after use was calcined in air at 400°C for 20 h, the surface area decreased slightly but remained higher than that of the fresh sample, indicating that the increase of surface area was not totally due to the deposition of coke.

1.2. X-Ray Diffraction

For Sb_2O_4 impregnated with Sn^{2+} or Sn^{4+} ions, only the peak characteristic of the support (Sb_2O_4) was observed. No shift of the peak position was detected. No difference was detected for this sample after catalytic reaction.

For SnO_2 impregnated with Sb ions, however, although no peaks were observed except those characteristic of SnO_2, all peaks shifted slightly to the right after impregnation (larger angle or smaller lattice parameter) with respect to pure SnO_2 (Figs. 1 and 2). The magnitude of the shift depended on the quantity of Sb ions in the sample; namely, the greater the quantity of Sb ions, the larger the shift (compare Fig. 1 with Fig. 2). In addition, the peaks became slightly broader and slightly asymmetrical. The shift of peak position decreased after reaction (compare the spectra before and after reaction). For $\frac{1}{2}Sb/SnO_2$, the spectrum after reaction is almost identical to that of pure SnO_2.

1.3. ^{119}Sn Mössbauer Spectroscopy

Due to the low quantity of SnO_2 (only 1.2 wt%) in the $1Sn^{2+}/Sb_2O_4$ sample, the Mössbauer spectrum was not as good as that of pure SnO_2, although it had been accumulated for almost 3 days. Nevertheless, the ^{119}Sn Mössbauer spectrum after the catalytic test showed only the presence of pure

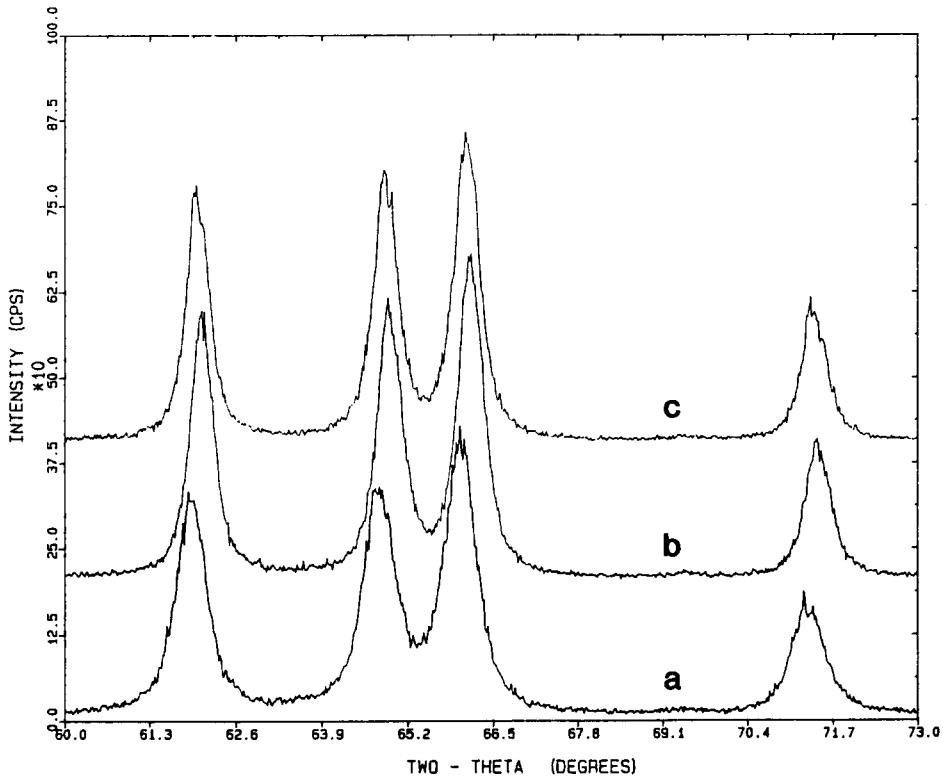

FIG. 2. X-ray diffraction spectra for $2Sb/SnO_2$, (a) SnO_2, (b) $2Sb/SnO_2$, and (c) $2Sb/SnO_2$ after reaction.

SnO_2 (Fig. 3) with IS = 0.02 mm/s and QS = 0.70 mm/s.

1.4. Electron Microscopy

Figures 4 and 5 present SEM pictures for $1Sn^{2+}/Sb_2O_4$ and $1Sb/SnO_2$, respectively.

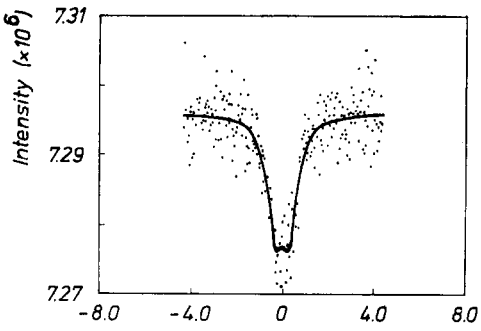

FIG. 3. ^{119}Sn Mössbauer spectrum for $1Sn^{2+}/Sb_2O_4$ after reaction (IS = 0.02, QS = 0.70 mm/s).

Compared with pure support oxides, no change has been observed from the point of view of surface morphology. This conclusion is valid even for the samples that had been used for catalysis.

The AEM spectra taken from $1Sn^{2+}/Sb_2O_4$ and $1Sb/SnO_2$ samples, respectively, are reported in Figs. 6 and 7. Within the sensitivity limits of the method, only the pure support oxides were detected in each case. The same conclusion has been reached for the samples after the catalytic test.

1.5. ESR

For the Sn/Sb_2O_4 samples, no ESR signal was observed for either the fresh or the used samples. However, a small signal with g = 1.8733 was observed for $1Sb/SnO_2$. The interesting point was that this signal decreased greatly (by almost 60%) after the sample had been used catalytically.

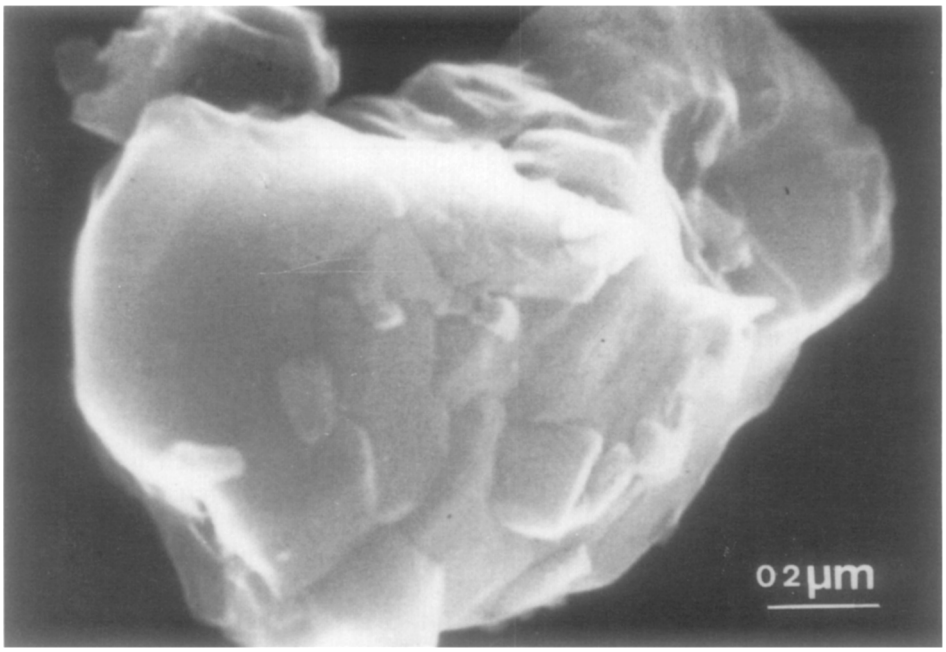

FIG. 4. SEM micrograph for $1Sn/Sb_2O_4$.

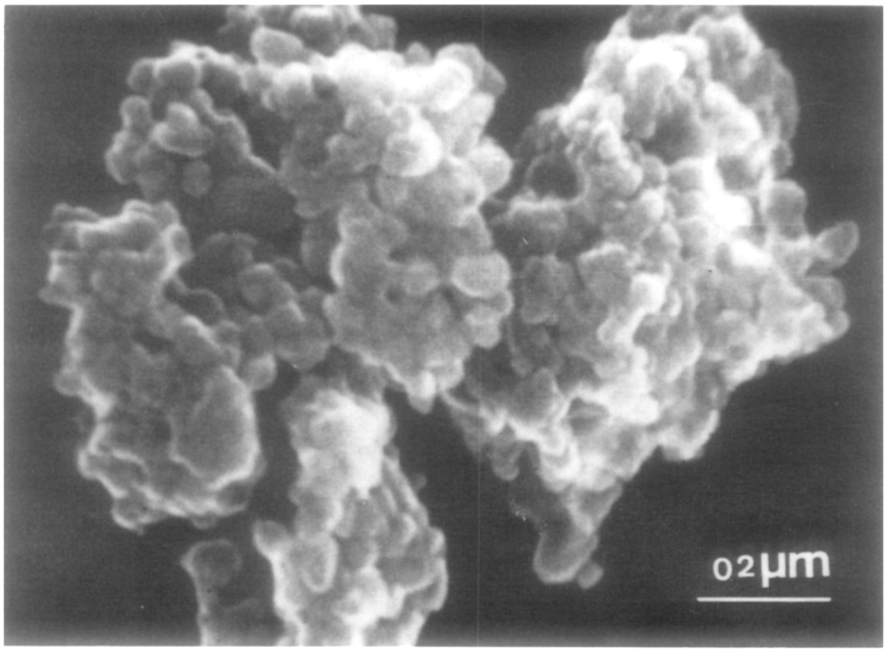

FIG. 5. SEM micrograph for $1Sb/SnO_2$.

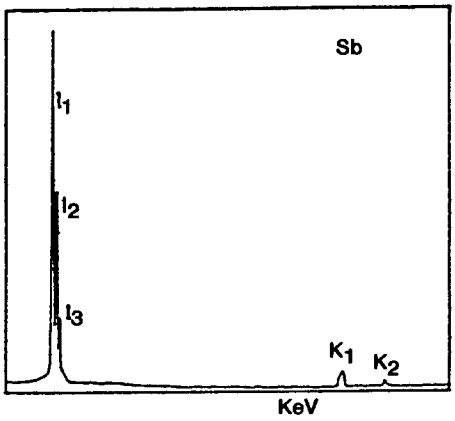

FIG. 6. AEM spectrum taken from $1Sn/Sb_2O_4$.

1.6. XPS

(*i*) *Sn/Sb_2O_4*. The binding energy values for $Sn_{3d_{5/2}}$ and $Sb_{3d_{3/2}}$ are 486.8 ± 0.2 eV and 540.0 ± 0.2 eV, respectively, for all samples. This corresponds to the values characteristic of pure oxides SnO_2 and Sb_2O_4 (*17–19*).

The value given for $Sb_{3d_{3/2}}$ is an average of $Sb(III)_{3d_{3/2}}$ and $Sb(V)_{3d_{3/2}}$. Our Vacuum Generators ESCA-3, as explained in Part I (*1*), does not permit us to distinguish with confidence the $Sb_{3d_{3/2}}$ lines of Sb(III) (539.6 eV) and Sb(V) (540.1 eV) due to the difference of charging effect of the two phases. We have tried to use the Auger parameter

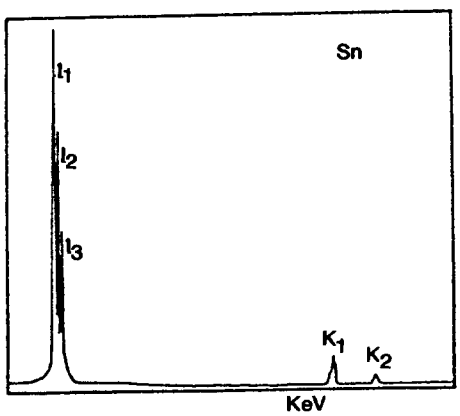

FIG. 7. AEM spectrum taken from $1Sb/SnO_2$.

TABLE 2

XPS Results for Sb_2O_4 Impregnated by Sn^{4+} Ions

Samples	C_{Sn}/C_{Si}	C_{Sb}/C_{Si}	$r_{XPS\text{-}Sn}$ [Sn/(Sb + Sn)]
$\frac{1}{2}Sn^{4+}/Sb_2O_4$	0.019	0.200	0.084
$\frac{1}{2}Sn^{4+}/Sb_2O_4$ (after test)	0.015	0.205	0.068
$1Sn^{4+}/Sb_2O_4$	0.046	0.209	0.180
$1Sn^{4+}/Sb_2O_4$ (after test)	0.032	0.202	0.137
$1Sn^{4+}/Sb_2O_4$ (400°C 6 h)	0.033	0.204	0.139
$1Sn^{4+}/Sb_2O_4$ (400°C 6 h + after test)	0.032	0.204	0.136
$2Sn^{4+}/Sb_2O_4$	0.064	0.169	0.275
$2Sn^{4+}/Sb_2O_4$ (after test)	0.052	0.175	0.229

($E_{k\,XPS} - E_{k\,Auger}$), which is insensitive to charge effects. Unfortunately, the Auger parameters are almost identical.

Table 2 presents the apparent relative concentrations C_{Sn}/C_{Si}, C_{Sb}/C_{Si}, and the surface composition index $r_{XPS\text{-}Sn}$ [Sn/(Sn + Sb)] for fresh and used samples, Sn^{4+}/Sb_2O_4. The results for $1Sn^{2+}/Sb_2O_4$ are not presented because they are similar to those of $1Sn^{4+}/Sb_2O_4$. From this table, it can be deduced that a large apparent concentration of Sn is present on the surface, representing almost 18% ($r_{XPS\text{-}Sn} \times 100\%$) for fresh $1Sn^{4+}/Sb_2O_4$. C_{Sn}/C_{Si} increases, while C_{Sb}/C_{Si} decreases slightly when the quantity of impregnated Sn^{4+} increases; $r_{XPS\text{-}Sn}$ also increases with increasing Sn^{4+}. In all cases, C_{Sn}/C_{Si} decreases greatly after catalytic reaction (e.g., 30% for $1Sn^{4+}/Sb_2O_4$) while C_{Sb}/C_{Si} remains almost constant; $r_{XPS\text{-}Sn}$ [Sn/(Sb + Sn)] decreases after the catalytic reaction.

For $1Sn^{4+}/Sb_2O_4$ after calcination at 400°C for 6 h, we observed the same diminution of $r_{XPS\text{-}Sn}$, indicating that the decrease in the Sn signal can also be provoked by thermal calcination. If this calcined sample (400°C, 6 h) was subsequently subjected to a catalytic test, however, almost no further diminution was observed.

Figure 8 shows the XPS intensity ratios (I_{Sn}/I_{Sb}) as a function of the theoretical number of SnO_2 monolayers on Sb_2O_4 for the fresh and used samples. For comparison, the theoretical I_{Sn}/I_{Sb} values for monolayer

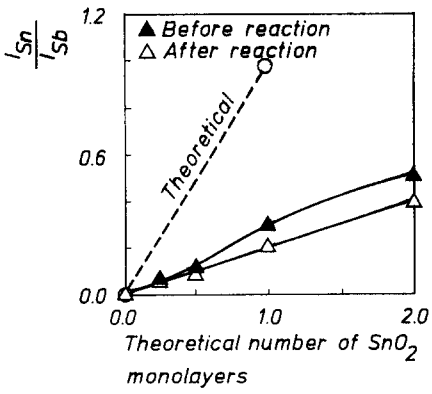

FIG. 8. XPS intensity ratio I_{Sn}/I_{Sb} as a function of the theoretical number of SnO_2 monolayers for the Sn/Sb_2O_4 samples.

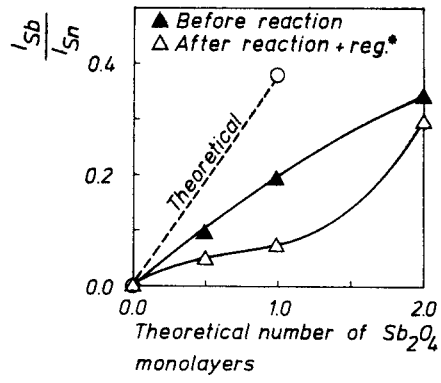

FIG. 9. XPS intensity ratio I_{Sb}/I_{Sn} as a function of the theoretical number of Sb_2O_4 monolayers for the Sb/SnO_2 samples.

formation when SnO_2 loading is lower than one monolayer are also presented. From this figure, conclusions the same as those taken from Table 2 can be obtained, namely that the Sn XPS signal increases with the Sn^{4+} quantity added and this signal decreases very significantly after reaction. Another interesting observation from this figure is that the experimental $\mathbf{I_{Sn}/I_{Sb}}$ values are much lower than those given by theory for effective monolayer formation.

(ii) Sb/SnO₂. The binding energies for $Sn_{3d_{5/2}}$ and $Sb_{3d_{3/2}}$ are identical, to a precision of ±0.2 eV, in all samples and correspond to those characteristic of the SnO_2 and Sb_2O_4 pure oxides.

Table 3 shows the apparent relative concentrations C_{Sn}/C_{Si}, C_{Sb}/C_{Si}, and the surface composition index $r_{XPS\text{-}Sb}$ [Sb/(Sn + Sb)] for this system. Sb is observed for all samples (presenting almost 20% ($r_{XPS\text{-}Sb}$ × 100%) of the surface for 1Sb/SnO_2), and C_{Sb}/C_{Si} increases with the quantity of Sb added during preparation. For the samples after catalytic reaction, not only C_{Sb}/C_{Si} but C_{Sn}/C_{Si} also decreases greatly. The C_{1s} peak also increases. However, when the samples were calcined, the Sn apparent relative concentration almost regained its initial value. Therefore, if we return to Sb and compare the $r_{XPS\text{-}Sb}$ values for the fresh samples and those measured after reaction and calcination (namely, if we eliminate the influence of the deposition of coke on the XPS results), we can conclude that $r_{XPS\text{-}Sb}$ [Sb/(Sn + Sb)] diminishes after reaction for all samples.

TABLE 3

XPS Results for SnO_2 Impregnated by Sb Ions

Samples	C_{Sn}/C_{Si}	C_{Sb}/C_{Si}	$r_{XPS\text{-}Sb}$ [Sb/(Sn + Sb)]
½Sb/SnO_2	0.544	0.071	0.115
½Sb/SnO_2 (after test)	0.300	0.037	0.110
½Sb/SnO_2 (test + reg.)[a]	0.546	0.038	0.065
1Sb/SnO_2	0.468	0.123	0.208
1Sb/SnO_2 (after test)	0.375	0.039	0.094
1Sb/SnO_2 (test + reg.)	0.460	0.046	0.091
2Sb/SnO_2	0.377	0.176	0.318
2Sb/SnO_2 (after test)	0.162	0.142	0.467
2Sb/SnO_2 (test + reg.)	0.380	0.152	0.286

[a] Reg. means the calcination in air at 400°C for 20 h.

Figure 9 shows the XPS intensity ratio $\mathbf{I_{Sb}/I_{Sn}}$ as a function of the quantity of Sb deposited on SnO_2, expressed as the theoretical number of monolayers. The theoretical values for loadings lower than 1 monolayer (calculated with Eq. (1)), and the experimental results for fresh samples and for used ones after calcination (in order to avoid the influence of coke) are shown. It can be observed that the experimental curve for fresh samples deviates from the theoreti-

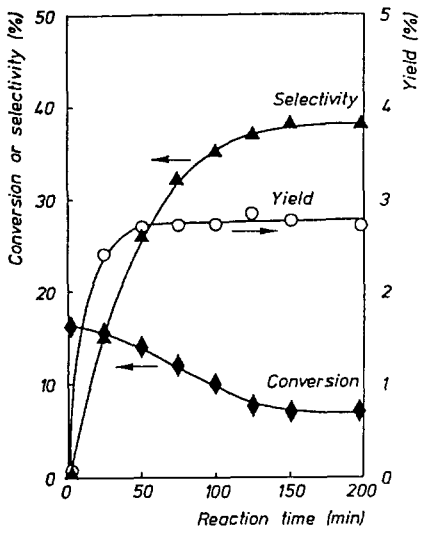

FIG. 10. Catalytic activity and selectivity as a function of reaction time for $1Sn^{2+}/Sb_2O_4$ at 400°C.

cal one at the beginning. The I_{Sb}/I_{Sn} values decrease after catalytic reaction.

2. CATALYTIC ACTIVITY

2.1. Sb_2O_4 Impregnated by Sn^{2+} or Sn^{4+}

(a) Change of the catalytic activity with time-on-stream. Figure 10 presents the variations of the overall conversion of isobutene, methacrolein yield, and selectivity as a function of time-on-stream at 400°C for $1Sn^{2+}/Sb_2O_4$. It can be observed that the overall conversion decreases, while methacrolein yield and selectivity increase progressively with the reaction time. After about 2 h of working, the catalytic activity and selectivity remain constant.

In order to investigate whether the dependence of the activity and selectivity on time for $1Sn^{2+}/Sb_2O_4$ was due to the oxidation of Sn^{2+} to Sn^{4+}, Sn^{4+}/Sb_2O_4 samples were also tested. The catalytic activity and selectivity for $1Sn^{4+}/Sb_2O_4$ are presented in Fig. 11. Almost the same behavior is observed; namely, the methacrolein yield and selectivity increase while the isobutene conversion decreases with reaction time for the first 2 h of working. Thereafter they are independent of reaction time. A similar behavior has been observed for the other samples, composed of Sn^{4+} impregnated on Sb_2O_4. The variation of the catalytic activity of the samples as a function of reaction time depends on the Sn^{4+} quantity added. The higher the Sn^{4+} content, the longer it took to attain a stable activity.

If another portion of $1Sn^{4+}/Sb_2O_4$ was calcined at 400°C for 6 h and was subsequently tested, the activity and selectivity (methacrolein yield = 2.9% and selectivity = 48%, values that are equal to those of $1Sn^{4+}/Sb_2O_4$ after stabilization of activity) were independent of reaction time.

(b) Influence of the quantity of impregnated Sn^{4+}. Figure 12 presents the stationary catalytic activity and selectivity, i.e., after at least 2 h of work, as a function of the Sn^{4+} quantity added. It can be observed that the catalytic activity (conversion and yield) increases while the selectivity to methacrolein decreases when the Sn^{4+} quantity increases. The methacrolein yield for $2Sn^{4+}/Sb_2O_4$ is almost equal to that of

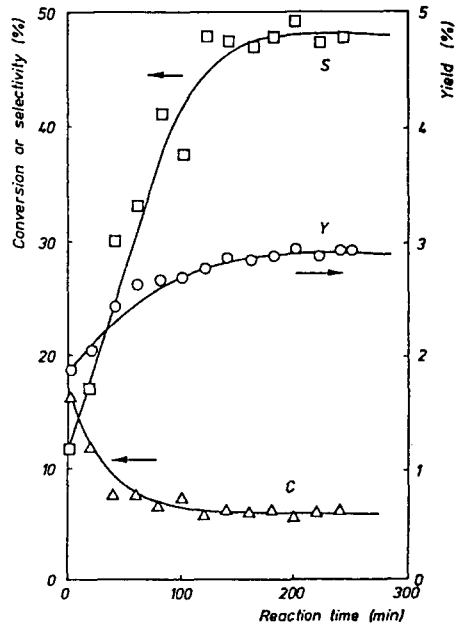

FIG. 11. Catalytic activity and selectivity as a function of reaction time for $1Sn^{4+}/Sb_2O_4$ at 400°C.

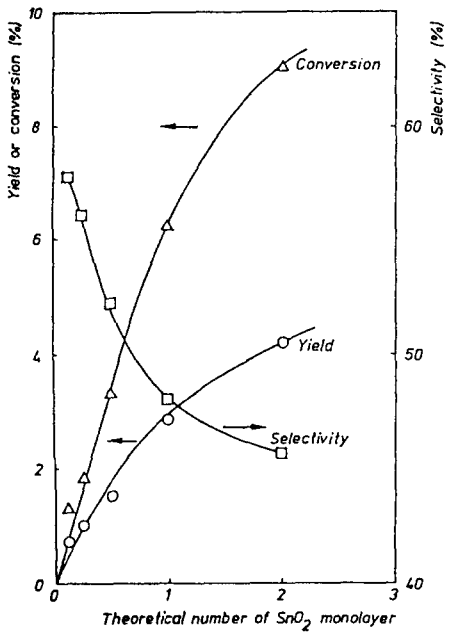

FIG. 12. Influence of the quantity of impregnated Sn^{4+} on the catalytic activity and selectivity of Sn^{4+}/Sb_2O_4 at 400°C.

the best mechanical mixture SnO_2(I)–Sb_2O_4 $R_m = 0.5$ (noted as M^I_{50}) (*1*) but with a much better selectivity (45% for $2Sn^{4+}/Sb_2O_4$ and 25% for M^I_{50}).

2.2. *SnO_2 Impregnated by Sb^{3+} and Sb^{5+}*

(*a*) *Change of catalytic activity with time-on-stream.* Figure 13 shows the variation of methacrolein yield and selectivity with reaction time at 400°C. Both yield and selectivity are independent of reaction time. The same behavior has been observed for the other Sb/SnO_2 samples.

(*b*) *Influence of the quantity of impregnated Sb ions.* Figures 14a, 14b, and 14c present the variation of the overall conversion of isobutene, methacrolein yield, and selectivity with the theoretical number of Sb_2O_4 monolayers on SnO_2 at 400 and 420°C, respectively (the results of pure SnO_2 were obtained using 400 mg then multiplying by 2 for conversion and yield (*1*)).

Compared with pure SnO_2, the impregnation of Sb ions first strongly decreases the overall conversion, but the addition of increasing amounts of Sb ions leads to a progressive recovery of conversion (Fig. 14a).

The methacrolein yield (Fig. 14b) and selectivity (Fig. 14c) increase with the quantity of Sb ions on the SnO_2 surface. Yields and selectivities are higher at higher reaction temperatures.

It is interesting to note that $2Sb/SnO_2$ gives almost the same conversion as pure SnO_2, while the methacrolein yield is almost 20 times greater! The methacrolein yield and selectivity of $1Sb/SnO_2$ are comparable to that of the best mechanical mixture M^I_{50} (*1*).

DISCUSSION

The activity results show that the catalytic properties of SnO_2 or Sb_2O_4 can be greatly improved by impregnation with a small amount of the other metallic ions.

The discussion must follow the same general lines as that of the previous article (*1*), because the issues are fundamentally similar. It will be necessary, in particular, to reexamine the possibility of mutual contamination of the phases, or formation of a solid solution. The possibility that a remote con-

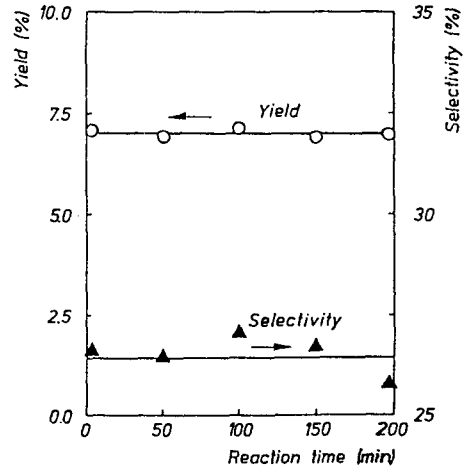

FIG. 13. Catalytic activity and selectivity as a function of reaction time for $1Sb/SnO_2$.

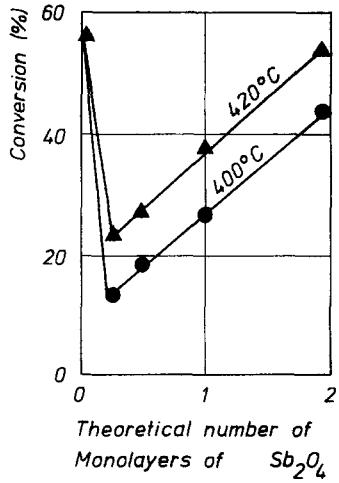

FIG. 14a. Isobutene conversion at 400°C and 420°C as a function of the quantity of Sb impregnated.

trol operates will be considered carefully. Indeed, if the artificially created contamination layer breaks down during catalytic reaction, small crystallites of the oxide of the impregnated element in very close contact with the "support" will form, and theoretically very favorable conditions would exist for transfer of spillover species between these phases.

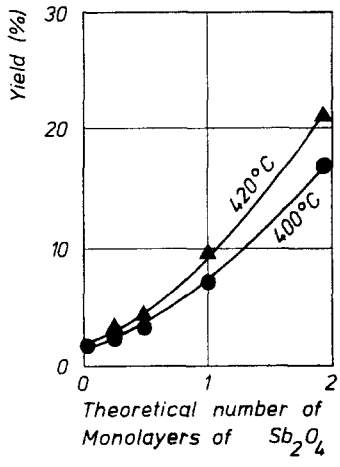

FIG. 14b. Methacrolein yield at 400°C and 420°C as a function of the quantity of Sb impregnated.

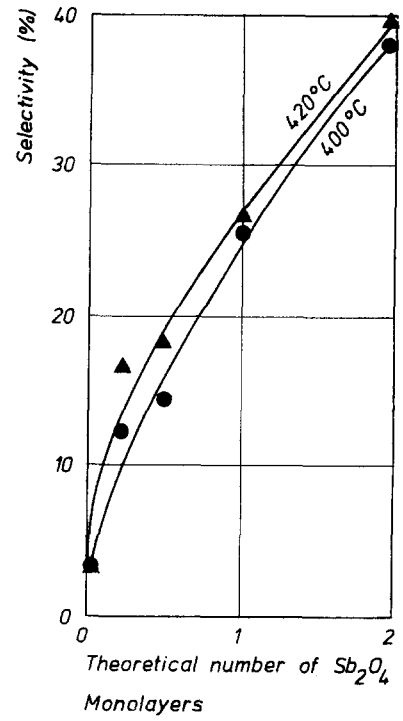

FIG. 14c. Methacrolein selectivity at 400°C and 420°C as a function of the quantity of Sb impregnated.

1. ARCHITECTURE OF THE IMPREGNATED CATALYSTS

1.1. Monolayer Formation

As mentioned in the experimental part, the impregnation method was employed in an attempt to form a layer of molecular thickness of one oxide over the other. The question is whether this layer (monolayer or fraction of a monolayer) was really formed.

Demonstrating the formation of a monolayer is not an easy task because of the low quantity of impregnated oxide (due to the low surface area of support oxide). The only technique useful for detecting the covering of an oxide by foreign elements is, in our case, XPS. For Sn/Sb_2O_4, the experimental values of I_{Sn}/I_{Sb} are much smaller than those given by the theoretical calculation for monolayer formation (Fig. 8), indicating that Sn does not spread as a layer of one molecule thickness over Sb_2O_4. The XPS

data, however, do not exclude that an imperfect contamination layer could form, e.g., that small crystallites, thicker than a monolayer, could adhere relatively strongly to the surface. After catalytic work (or thermal calcination), however, $r_{XPS\text{-}Sn}$ [Sn/(Sn + Sb)] decreases greatly. This indicates that this imperfect layer (if it exists) "shrinks" extensively, leaving free much more of the Sb_2O_4 surface. A similar conclusion can be obtained from Fig. 9 and Table 3 for the other samples; namely, Sb/SnO_2: Sb does not form a perfect monolayer over SnO_2 and the Sb ions leave free a large part of the surface of SnO_2 during reaction.

1.2. Formation of a Solid Solution

For Sb_2O_4 impregnated by Sn ions, XRD shows no shift of the peak position and no signal is observed by ESR in any sample. This shows that, within the sensitivity limit of the technique, no solid solution is formed during either preparation or catalytic reaction.

For SnO_2 impregnated by Sb ions, however, XRD measurements show that the SnO_2 peak positions shift to the right (higher angle) after impregnation. This indicates that some Sb^{5+} ions are dissolved into SnO_2. We observed an ESR signal at $g = 1.8733$ for sample $1Sb/SnO_2$. This confirms that Sb^{5+} ions are dissolved in SnO_2 (*9*). The small enlargement and the asymmetry of the XRD peaks indicate, in addition, that the composition of Sb on SnO_2 is heterogeneous. This is understandable: the top layers of SnO_2 have dissolved Sb, whereas the core remains unaltered, and this corresponds to different lattice spacings. More Sb^{5+} ions are incorporated into SnO_2 when the Sb loading is increased (greater shift to a higher reflection angle, i.e., smaller lattice parameter).

An important phenomenon is that the shift of the SnO_2 lines decreases and the peaks become more symmetrical after reaction. This may be the consequence of two possible processes: (i) homogenization of the dissolved Sb ions or (ii) segregation of the dissolved Sb ions from SnO_2. The latter is more plausible because the ESR signal corresponding to the dissolution of Sb^{5+} in SnO_2 decreases. The conclusion is that Sb^{5+} ions can be dissolved into the SnO_2 lattice during preparation, but that they migrate to the surface of SnO_2 and segregate during the catalytic test. In addition, the Sb/(Sb + Sn) ratio decreases after reaction. This shows that the impregnated ions crystallize with a loss of dispersion to antimony oxide during the catalytic reaction.

1.3. Evolution of the Architecture of the Catalysts during the Catalytic Reaction: Formation of Small Crystallites of Deposited Phase

(*i*) *Sn/Sb_2O_4*. For Sb_2O_4 impregnated by Sn^{2+} or Sn^{4+}, the fact that $r_{XPS\text{-}Sn}$ [Sn/(Sb + Sn)] decreases indicates that the oxide containing the impregnated Sn ions (Sn^{2+} or Sn^{4+}) loses dispersion during the catalytic reaction or thermal calcination. We can thus expect to have indications of the formation of small crystallites of the SnO_2 phase. Indeed, we observe a ^{119}Sn Mössbauer spectrum characteristic of SnO_2 for $1Sn^{2+}/Sb_2O_4$ after reaction. In addition, if SnO_2 is spread as a monolayer, or thin layers, the BET surface area of the impregnated Sb_2O_4 should remain essentially the same as that of pure Sb_2O_4, but the formation of the small crystallites should correspond to the creation of a new surface area. This is indeed what we observe (Table 1). The fact that we cannot observe the presence of SnO_2 crystallites in SEM is due to the fact that the crystallites are too small, as could be expected from the fact that they create an appreciable surface area.

One can thus summarize the evolution of the architecutre of Sn/Sb_2O_4 system as represented in Fig. 15a.

(*ii*) *Sb/SnO_2*. The situation of Sb/SnO_2 is more complicated owing to the formation of a solid solution. However, similar observations have been made, namely that $r_{XPS\text{-}Sb}$ [Sb/(Sn + Sb)] decreases, and the BET surface increases after reaction. Taking into

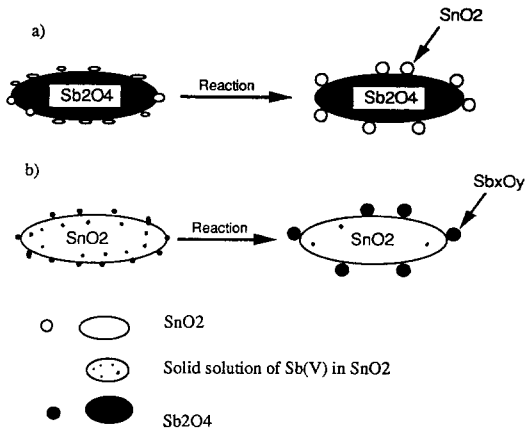

FIG. 15. Changes during catalytic reaction of (a) Sn/Sb_2O_4 and (b) Sb/SnO_2.

account the results presented and discussed above, the evolution of the architecture of this system can be summarized as represented as in Fig. 15b.

Our results agree with two sets of results published in the literature. Sb ions tend to migrate toward the surface of SnO_2 samples doped with Sb (<5 at.%) calcined at extremely high temperature (oxide coating in ceramics) as shown by Auger spectroscopy, XPS, UPS, and HREELS (*20, 21*). Similarly, Volta *et al.* (*22*) studied SnO_2 impregnated by Sb ions and calcined at 500°C. On the basis of electrical conductivity measurements, the authors concluded that only a small amount of impregnated Sb ions was incorporated into SnO_2 to form a solid solution; using IR spectroscopy they found that an antimony compound was present as a deposit on SnO_2.

In conclusion, the impregnated catalysts tend to segregate to form *two-phase* catalysts. This is true even when some solid solution is formed. A similar conclusion has been obtained for the MoO_3–Sb_2O_4 system (except that there is no solid solution) (*23*). Taking also into account the results obtained with the mechanical mixtures (*1, 23*), our conclusion is that the stable thermodynamic state at reaction temperature and under the reaction conditions corresponds to the existence of biphasic catalysts (MoO_3 + Sb_2O_4 and SnO_2 + Sb_2O_4 or $Sb_xSn_{1-x}O_2$ (solid solution) + Sb_2O_4). This is a situation completely different from that of systems such as V_2O_5–TiO_2, V_2O_5–ZrO_2, V_2O_5–Al_2O_3, MoO_3–TiO_2, MoO_3–Co_3O_4, and MoO_3–Mn_2O_3 (*24, 25*), where a spontaneous contamination takes place.

2. Correlation of Activity with the Architecture and Physico-chemical Properties of the Catalysts

(*1*) *Sn/Sb_2O_4*

With Sn/Sb_2O_4 the methacrolein yield and selectivity increase while conversion decreases during the first 2 h of working (Figs. 10 and 11). The stable activity of Sn/Sb_2O_4 samples (after 2 h of working) corresponds to catalysts composed of small crystallites of SnO_2 on the surface of Sb_2O_4.

Supposing that the synergy is due to contamination, we should observe a decrease of catalytic activity during catalytic reaction. This goes against our experimental results. On the other hand, $2Sn/Sb_2O_4$, whose Sn content is two times greater than that necessary to form a monolayer, shows catalytic properties much better than those of $1Sn/Sb_2O_4$. This suggests that the origin of activity is not monolayer formation (or minute contamination). No solid solution was detected. The increase of activity is linked to the formation of separate SnO_2 crystallites. This effect corresponds to what would be expected if a remote control effect operated: small crystallites of the active phase (acceptor: SnO_2) must be formed, and a sufficient surface area of the donor (Sb_2O_4) must be set free for producing spillover oxygen.

(*2*) *Sb/SnO_2*

The situation with Sb/SnO_2 is different. The catalytic activity is independent of reaction time. The stable activity corresponds to a catalyst composed of small crystallites of antimony oxide on the surface of SnO_2 and a small amount of solid solution. Similar

to the other system, we observe an evolution of the architecture of the catalysts during the reaction. A dependence of catalytic activity on reaction time should normally be observed. The surprising results we observed may be explained if we suppose that this evolution is very rapid or even takes place during the preheating of the catalyst.

There is no doubt that antimony oxide segregates during reaction. The problem is whether the small amount of solid solution that remains could explain the good activity and selectivity of the Sb/SnO_2 catalysts. The solid solution has been proposed by Godin *et al.* (*26*) to be the active phase in their coprecipitated Sn–Sb–O catalysts. However, the validity of this assumption has not yet been totally proven (*27, 28*) and is indeed seriously questioned (*29*). In our case, the assumption that the solid solution (Sb^{5+} dissolved in SnO_2) constitutes the active phase in Sb/SnO_2 system cannot be absolutely ruled out. However, this explanation faces serious objections. On one hand, the characterization results with XRD and ESR show that the solid solution formed during impregnation is not stable during the catalytic reaction, namely that Sb^{5+} ions migrate to the surface. On the other hand, if we compare the methacrolein yield of $\frac{1}{4}Sb/SnO_2$ with that of $2Sb/SnO_2$, we come to the conclusion that the improvement of methacrolein yield depends on the increase of the amount of segregated antimony oxide rather than on the number of Sb^{5+} ions associated with SnO_2.

The stable state of this system corresponds to the existence of two phases, either $Sb_xO_y + SnO_2$ or $Sb_xO_y + Sb_xSn_{1-x}O_2$ (solid solution). It is thus logical to consider the cooperation between these phases when trying to identify the origin of the synergy. Part III of this series (*30*) dealing with a solid solution (e.g., 5 at.% of Sb) prepared by the coprecipitation method, and mixed mechanically with pure Sb_2O_4, prepared separately, will show that a conspicuous synergy still exists. This will indicate that, even if the solid solution is considered as important, phase cooperation does play an additional role, thus strengthening the present conclusions.

3. Detailed Explanation of the Catalytic Activity Results within the Framework of the Remote Control Mechanism

The existence of two separate phases in the catalysts that have adjusted their architecture during the catalytic reaction lead us naturally to present the remote control as the explanation of the catalytic performances improvement (selectivity and yield in methacrolein), as we did in other cases of two-phase catalysts [e.g., Refs. (*1, 23*)].

Concerning Sn/Sb_2O_4 catalysts, we indicated above that the increase of Sn content (namely of sites potentially active if properly irrigated by spillover oxygen) and/or the fact that the surface of Sb_2O_4 became free (namely able to produce spillover oxygen) were two favorable factors for a better and more efficiently activated ("controlled") catalyst to be formed (Figs. 10–12). The same conclusion can be reached with Sb/SnO_2, without having to decide for the moment whether SnO_2 or the $Sb_xSn_{1-x}O_2$ solid solution is the acceptor.

In comparison with the mechanical mixtures discussed in Ref. (*1*), the impregnated catalysts possess surprisingly high performances. For instance, the methacrolein yield with $1Sb/SnO_2$ is comparable to that of the best mechanical mixture M^{I}_{50}, although the amount of Sb is very small (4 wt%). It is interesting to see whether a comparison of the surface areas developed by each phase in these two categories of catalysts, in the light of the remote control mechanism, could explain, qualitatively at least, the results. Let us compare the results of the best mechanical mixture, M^{I}_{50}, with those of $1Sn/Sb_2O_4$ (Table 4). For that, it is necessary to estimate the size of the SnO_2 crystallites in $1Sn/Sb_2O_4$. The length (c) of the edge of the SnO_2 crystallites (supposed

TABLE 4

Comparison of the Physico-chemical Characteristics and Catalytic Activity between M^{I}_{50} and $1Sn/Sb_2O_4$

Sample	Physico-chemical characteristics						Catalytic activity	
	SnO_2 wt%	Method	Cubic length of SnO_2 (nm)	Specific surface of SnO_2 ($m^2\ g^{-1}$)	Total surface of SnO_2 ($m^2\ g^{-1}$)	Total surface of Sb_2O_4 ($m^2\ g^{-1}$)	Yield (%)	Selectivity (%)
$1Sn/Sb_2O_4$	1.2	XPS	5.5	157.0	1.88	2.00	2.9	48
	1.2	BET		83.0	1.00	2.00	2.9	48
M^{I}_{50}	50.0	BET		12.6	6.30	1.00	5.0	25

to be cubic) can be calculated from the XPS results, using Eq. (2). The specific surface area and total surface area for these crystallites are calculated both from their size c and from the BET surface area results, assuming that the difference of the surface area before and after catalytic reaction is due to the contribution of the surface area developed by the SnO_2 crystallites (Table 1). SnO_2 develops a surface area in $1Sn/Sb_2O_4$ lower (between 1 and 1.9 $m^2\ g^{-1}$) than that in M^{I}_{50} (6.3 $m^2\ g^{-1}$). It is thus not surprising that the yield in methacrolein is smaller in absolute value. However, per unit surface area it is 2 to 3.5 times higher (2.9 : 1 or 2.9 : 1.9 compared to 5 : 6.3); namely, SnO_2 carries more selective centers. There is approximately twice as much free Sb_2O_4 surface in $1Sn/Sb_2O_4$ as in M^{I}_{50}. Consequently, more spillover oxygen is available. In addition, the crystallites of SnO_2 are much smaller, and spillover oxygen can more easily reach all their surface. The surface of SnO_2 is better irrigated with spillover oxygen, resulting in a larger proportion of the sites being selective (last column of Table 4). Similar arguments could be developed to explain the good methacrolein yields and selectivity obtained with Sb/SnO_2.

This simple calculation shows that the results are those that would be expected if a remote control operates.

In conclusion, although we cannot absolutely exclude the possibility that a minute contamination or the formation of a solid solution could explain part of the observed effects, there are strong arguments for believing that a cooperation between different phases takes place, and that this cooperation is a remote control.

CONCLUSIONS

- The catalytic properties of SnO_2 or Sb_2O_4 can be greatly improved by impregnating a small amount of the cation belonging to the other oxide (Sb^{3+}/Sb^{5+} for SnO_2 and Sn^{2+} or Sn^{4+} for Sb_2O_4).
- A small amount of Sb^{5+} ions can be dissolved in SnO_2 in Sb/SnO_2 catalysts. However, these ions migrate to the surface during the catalytic oxidation of isobutene.
- For both Sb/SnO_2 and Sn/Sb_2O_4, the impregnated ions tend to crystallize on the oxide support. The result is the formation of two-phase catalysts during the catalytic reaction.
- These results and the comparison between the catalytic activities of the catalyst and the surface areas developed, respectively, by each phase in the impregnated catalysts and the mechanical mixtures are consistent with the existence of a remote control mechanism.

ACKNOWLEDGMENTS

We gratefully thank the Université Catholique de Louvain and the Chinese Government for financial sup-

port for one of us (L. T. Weng), and the Service de Programmation de la Politique Scientifique for supporting this line of research. We thank Dr. J. Naud for his help with the XRD measurements.

REFERENCES

1. Weng, L. T., Spitaels, N., Yasse, B., Ladrière, J., Ruiz, P., and Delmon, B., *J. Catal.* **132,** 319 (1991).
2. Machej, T., Remy, M., Ruiz, P., and Delmon, B., *J. Chem. Soc., Faraday Trans. 1* **86,** 715 (1990).
3. Haber, J., *in* "Surface Properties and Catalysis by Non-metals" (J. P. Bonnelle, B. Delmon, and E. Derouane, Eds.), p. 1, Nato ASI Series C105. Reidel, Dordrecht, 1983.
4. Bond, G. C., and König, P., *J. Catal.* **79,** 309 (1982).
5. Courtine, P., *in* "Solid State Chemistry and Catalysis" (R. K. Grasselli and J. P. Brazdil, Eds.), ACS Symposium Series 279, p. 37, 1985.
6. Andersson, A., and Andersson, S. L. T., *in* "Solid State Chemistry and Catalysis" (R. K. Grasselli and J. P. Brazdil, Eds.), ACS Symposium Series 279, p. 121, 1985.
7. Wachs, I. E., Chan, S. S., and Saleh, R. Y., *J. Catal.* **91,** 3 (1985).
8. Bond, G. C., Zurita, J. P., Flamerz, S., Gellings, P. J., Bosch, H., van Ommen, J. G., and Kip, B. J., *Appl. Catal.* **22,** 361 (1986).
9. Berry, F. J., and McAteer, J. C., *Inorg. Chim. Acta.* **50,** 85 (1981).
10. Roginskaya, Yu. E., Dulin, D. A., Stroeva, S. S., Kul'kova, N. V., and Gel'bshtein, A. I., *Kinet. Katal.* **9,** 1143 (1968).
11. Wright, D. A., *Proc. Br. Ceram. Soc.* **10,** 103 (1968).
12. Gopalakrishnan, P. S., and Manohar, H., *Cryst. Struct. Commun.* **4,** 203 (1975).
13. Wagner, C. D., Davis, L. E., Zeller, H. V., Taylor, P. A., Raymond, R. H., and Gale, L. H., *Surf. Interface Anal.* **3,** 21 (1981).
14. Kerkhof, E. P. J. M., and Moulijn, J. A., *J. Phys. Chem.* **83,** 1612 (1979).
15. Scofield, J. H., *J. Electron Spectrosc. Relat. Phenom.* **8,** 29 (1976).
16. Szajman, J., Liesegang, J., Jenkin, J. G., and Leckey, R. C. C., *J. Electron Spectrosc. Relat. Phenom.* **23,** 97 (1981).
17. Birchall, T., Connor, J. A., and Hillier, I. H., *J. Chem. Soc. Dalton,* 2003 (1975).
18. Boudville, Y., Figueras, F., Forissier, M., Portefaix, J. L., and Védrine, J. C., *J. Catal.* **58,** 52 (1979).
19. Cross, J. M., and Pyke, D. R., *J. Catal.* **58,** 61 (1979).
20. Cox, P. A., Egdell, R. G., Harding, C., Patterson, W. R., and Taverner, P. J., *Surf. Sci.* **123,** 179 (1982).
21. Hennaut, M. F., Duvigneaud, P. H., and Plumat, E., *Silic. Ind.* **9,** 171 (1984).
22. Volta, J. C., Bussière, P., Coudurier, G., Herrmann, J. M., and Védrine, J. C., *Appl. Catal.* **16,** 315 (1985).
23. Weng, L. T., Zhou, B., Yasse, B., Doumain, B., Ruiz, P., and Delmon, B., *in* "Proceedings, 9th International Congress on Catalysis, Calgary, 1988" (M. J. Phillips and M. Ternan, Eds.), Vol. 4, p. 1609. Chem. Institute of Canada, Ottawa, 1988.
24. Haber, J., *Pure Appl. Chem.* **56,** 1663 (1984).
25. Stampfl, S. R., Chen, Y., Dumesic, J. A., Niu, C. M., and Hill, C. G., Jr., *J. Catal.* **105,** 445 (1987).
26. Godin, G. W., McCain, C. C., and Porter, E. A., *in* "Proceedings, 4th International Congress on Catalysis, Moscow, 1968" (B. A. Kazansky, Ed.), Vol. 1, p. 271. Adler, New York, 1968.
27. Berry, F. J., *in* "Advances in Catalysis" (D. D. Eley, H. Pines, and P. B. Weisz, Eds.), Vol. 30, p. 97. Academic Press, New York, 1980.
28. Viswanathan, B., and Chokkalingam, S., *Surf. Technol.* **23,** 231 (1984).
29. Figueras, F., Forissier, M., Lacharme, J. P., and Portefaix, J. L., *Appl. Catal.* **19,** 21 (1985).
30. Weng, L. T., Patrono, P., Sham, E., Ruiz, P., and Delmon, B., *J. Catal.* **132,** 360 (1991).